PLANT SCIENCE

Hydraulic flux–responsive hormone redistribution determines root branching

Poonam Mehra[1]*, Bipin K. Pandey[1], Dalia Melebari[1], Jason Banda[1], Nicola Leftley[1], Valentin Couvreur[2], James Rowe[3], Moran Anfang[4], Hugues De Gernier[5,6], Emily Morris[1]†, Craig J. Sturrock[1], Sacha J. Mooney[1], Ranjan Swarup[1], Christine Faulkner[7], Tom Beeckman[5,6], Rishikesh P. Bhalerao[8], Eilon Shani[4], Alexander M. Jones[3], Ian C. Dodd[9], Robert E. Sharp[10], Ari Sadanandom[11], Xavier Draye[2], Malcolm J. Bennett[1]*

Plant roots exhibit plasticity in their branching patterns to forage efficiently for heterogeneously distributed resources, such as soil water. The xerobranching response represses lateral root formation when roots lose contact with water. Here, we show that xerobranching is regulated by radial movement of the phloem-derived hormone abscisic acid, which disrupts intercellular communication between inner and outer cell layers through plasmodesmata. Closure of these intercellular pores disrupts the inward movement of the hormone signal auxin, blocking lateral root branching. Once root tips regain contact with moisture, the abscisic acid response rapidly attenuates. Our study reveals how roots adapt their branching pattern to heterogeneous soil water conditions by linking changes in hydraulic flux with dynamic hormone redistribution.

Root branching determines foraging capacity of crop plants (*1*, *2*). Roots have evolved plasticity in their branching patterns to maximize access to soil water resources, which are often distributed heterogeneously (*3*, *4*). Root branching is affected both by extreme weather (such as drought or flooding) (*5*, *6*) and by transient or local spatial differences in soil moisture (*7*, *8*). Negative effects of water scarcity on modern agriculture will be exacerbated as climate change affects hydrological cycles and soil water resources (*9*, *10*). Increased resilience in the face of climate change will require better insight into how plant roots sense and adapt to fluctuating water availability.

Dissecting roots' water sensing using xerobranching

Xerobranching (*7*) provides an experimental model to study root adaptive responses to transient water stress. A xerobranching response is triggered when growing root tips temporarily lose contact with moist soil (e.g., in an air gap), which causes branching to temporarily cease until roots reenter moist soil (Fig. 1A). To discover the mechanistic basis of xerobranching, an agar-based xerobranching bioassay was developed (fig. S1) that phenocopies the original x-ray computed tomography (CT) soil-based bioassay (Fig. 1A) in experiments with *Arabidopsis* and tomato seedlings. As levels of the abiotic stress signal abscisic acid (ABA) increase in root tips during transient water stress (*7*), we tested whether tomato ABA biosynthesis mutants (*flacca* and *notabilis*) (*11*, *12*) are disrupted in xerobranching response. Both soil- and agar-based bioassays revealed that, unlike wild-type (WT) controls, primary roots of both *flacca* and *notabilis* continue to branch when growing across an air gap (Fig. 1, A to D, and fig. S2). Similarly, the ABA-deficient maize mutant *vp14* (*13*) disrupted xerobranching in both paper-based and soil-based bioassays (figs. S3 and S4). Hence, ABA is a widely conserved regulator that represses lateral root development during a xerobranching response in these monocot and eudicot plant models.

From which tissue(s) does ABA originate to trigger a xerobranching response? ABA biosynthesis genes, such as *ABA2*, are expressed in phloem-related root vascular tissues (*14*). *Arabidopsis aba2-1* mutant roots exhibit a xerobranching defect, which can be rescued by expressing WT *ABA2* using the phloem companion cell–expressed *SUC2* promoter (Fig. 1, E to G, and fig. S5A). A *SUC2:YFP-ABA2* translation fusion confirmed that the ABA2 protein can act in a phloem companion cell–autonomous manner (fig. S5B). Phloem provides water for growing roots in the temporary absence of an external supply (*15*). Hydraulic modeling (*16*, *17*) predicts that radial water fluxes within root tissues change direction from predominately inward to outward after a xerobranching stimulus (Fig. 1H). Simulations reveal that an inward water flux dominates under normal externally hydrated conditions, and phloem-derived water is limited to close to companion cells (Fig. 1H). However, after a xerobranching stimulus (when the external water source is temporarily lost), root-tip tissues rely on an outward flux of phloem-derived water to maintain growth, requiring ~8 hours for outer root tissues to receive phloem water (Fig. 1H). Phloem-derived ABA is likely to travel with this outward flow of water during a xerobranching response.

ABA moves outward after a xerobranching stimulus

To visualize whether, when, and where ABA movement occurs after a xerobranching stimulus, we used a sensitive Förster resonance energy transfer (FRET)–based hormone biosensor (*18*), nlsABACUS2, which displays increased fluorescence emission ratio upon ABA binding (fig. S6). Seedlings expressing a nuclear-localized nlsABACUS2 biosensor revealed dynamic changes in ABA distribution and levels during our agar-based xerobranching bioassay (Fig. 1, I to K, and figs. S7 and S8). Spatially, nlsABACUS2 accumulates in epidermal cells in the basal meristem and elongation zones (Fig. 1J). Quantifying temporal changes in emission ratios revealed that ABA levels initially increase in root epidermal tissues >12 hours after a xerobranching stimulus. Considering the sensitivity of the biosensor, these results are also consistent with our hydraulic simulations that predict the outward flux of phloem-derived water after ~8 hours of xerobranching stimulus (Fig. 1H). Once root tips reconnect with the agar (recovery phase), ABA levels fall rapidly in epidermal cells (Fig. 1, J and K, and fig. S8).

To directly visualize whether ABA moves radially outward ("piggy-backing" the redirection of water flux) after a xerobranching stimulus, we generated cross-sectional images of nlsABACUS2 root-tip tissues (Fig. 2) from three key zones. These zones included meristem and early elongation zone tissues (zone 1), mid- to late elongation and early differentiation zone tissues (zone 2), and fully differentiated root tissues (zone 3). Radial images of these three zones (taken at different time points during the xerobranching response) revealed contrasting patterns of ABA redistribution. For example, an increase in ABA levels can initially be detected in inner root tissues that is later seen in outer tissues in zone 2 (compare nlsABACUS2 signals in 3- versus 4-mm root-tip sections for zone 2 in Fig. 2), consistent with ABA movement from inner to outer root tissues. By contrast, radial cross sections through nlsABACUS2 zone 1 root tissues revealed an increase in ABA in outer (but not inner) tissues, which suggests that this signal originates from

[1]Plant and Crop Sciences, School of Biosciences, University of Nottingham, Nottingham, UK. [2]Earth and Life Institute, Université catholique de Louvain, 1348 Louvain-la-Neuve, Belgium. [3]Sainsbury Laboratory, University of Cambridge, Cambridge, UK. [4]School of Plant Sciences and Food Security, Tel Aviv University, Tel Aviv, Israel. [5]Department of Plant Biotechnology and Bioinformatics, Ghent University, 9052 Ghent, Belgium. [6]Center for Plant Systems Biology, VIB-UGent, 9052 Ghent, Belgium. [7]Crop Genetics, John Innes Centre, Norwich Research Park, Norwich, UK. [8]Umeå Plant Science Centre, Department of Forest Genetics and Plant Physiology, Swedish University of Agricultural Sciences, SE-901 87 Umeå, Sweden. [9]Lancaster Environment Centre, Lancaster University, Lancaster, UK. [10]Division of Plant Science and Technology, University of Missouri, Columbia, MO, USA. [11]Department of Biosciences, University of Durham, Durham, UK.
*Corresponding author. Email: p.mehra@nottingham.ac.uk (P.M.); malcolm.bennett@nottingham.ac.uk (M.J.B.)
†Present address: Oxford University Innovation, Oxford, UK.

phloem unloading in zone 2 and then undergoes redistribution through symplastic continuity. ABA accumulated much less in outer root tissues of zone 3 versus zones 1 and 2 after a xerobranching stimulus (Fig. 2). The results are consistent with the phloem unloading patterns of solutes described earlier (*19*), which suggests that zone 2 overlaps with the protophloem unloading zone, where solutes are transferred laterally through symplastic continuity. By contrast, zone 3 is active in solute translocation through phloem but inactive in phloem unloading (*19*). Another parallel study also reports similar expression patterns of nlsABACUS when exogenously applied ABA unloads through phloem (*18*). The pattern of elevated ABA in outer root tissues of zones 1 and 2 also coincides with the root-tip region, where new lateral root primordia initiate (termed the basal meristem or oscillatory zone) (*20*, *21*). Elevated levels of ABA in zones 1 and 2 rapidly decrease once root-tip tissues contact a new moisture source during the recovery phase (Fig. 2). Endogenous ABA levels in cotyledons of nlsABACUS2 plants did not change after a xerobranching stimulus, which suggests that ABA accumulation is locally confined to root tips that are exposed to air gaps (figs. S7 to S9). Hence, during a xerobranching response, ABA accumulates in the root zone that is associated with the earliest stage of lateral root development.

To test the function of the observed changes in ABA after a xerobranching stimulus, we examined the impact of mutations in key components of the ABA signaling machinery for this adaptive response. ABA-insensitive mutants disrupting ABA receptors (*pyr/pyl*) and ABA-activated SnRK2 kinases (*snrk2.2/2.3*, *snrk2.2/2.3/2.6*) exhibited lateral root branching in our xerobranching bioassay (Fig. 3A and figs. S10 and S11), whereas ABA-hypersensitive *pp2c* mutants failed to produce lateral roots in the air gap (fig. S12). Detailed analysis with *snrk* triple, septuple, and nonuple mutants as well as *snrk2.2* complementation lines revealed that *SnRK2.2* is required for xerobranching (Fig. 3D and fig. S11). Roots of a *snrk* nonuple mutant (which lacked 9 of 10 members of the SnRK2 family except SnRK2.2) behaved like WT in our xerobranching bioassay (fig. S11). Furthermore, a green fluorescent protein (GFP)–tagged SnRK2.2 reporter *pSnRK2.2:SnRK2.2-GFP* revealed that a xerobranching stimulus induced the fusion protein in the basal root meristem (Fig. 3, B and C, and fig. S13), which overlaps with the site of largest emission ratio changes of the ABA biosensor nlsABACUS2 (Fig. 1J). Hence, SnRK2.2 regulates ABA (and in turn, the xerobranching) response in *Arabidopsis* root tissues.

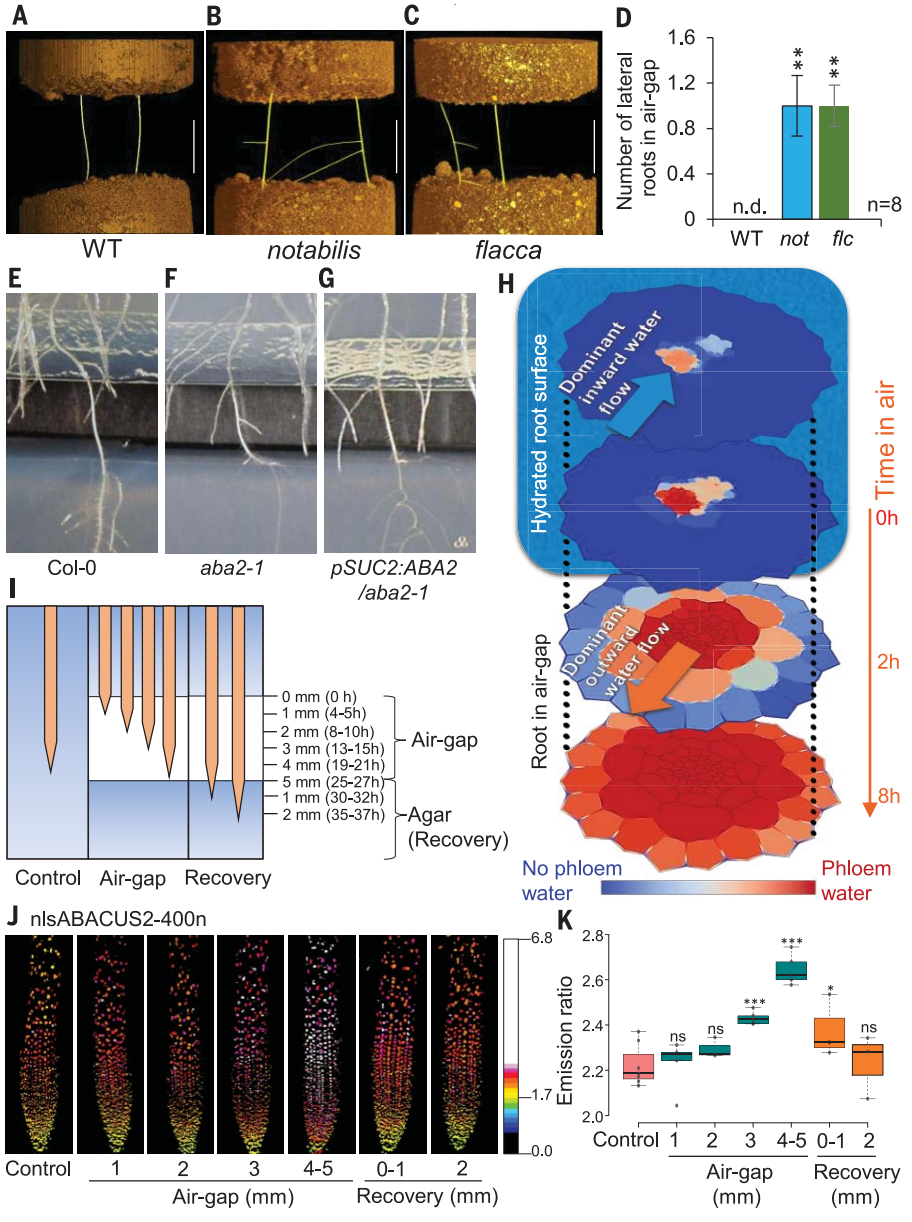

Fig. 1. ABA functions as a repressive signal during xerobranching response. (**A** to **D**) Representative CT images [(A) to (C)] and a bar graph (D) showing xerobranching defect in ABA-deficient tomato mutants (*notabilis* and *flacca*) versus WT (Ailsa Craig). Air gap, ~1.5 cm. Scale bar, 1 cm. n.d., not detected. (**E**) Agar-based air-gap assay system showing xerobranching response in *Arabidopsis* WT (Col-0) (air gap, ~5 mm). (**F**) *Arabidopsis* ABA biosynthetic mutant *aba2* produces lateral roots in air gap. (**G**) Expression of *ABA2* in phloem companion cells rescues xerobranching defect of *aba2*. (**H**) The MECHA hydraulic model predicts phloem as the main source of water in *Arabidopsis* root elongation zone only when located in an air gap. Simulated water advection maps show dominating phloem water in root epidermal cells within 8 hours. (**I**) For studying temporal response of reporters during xerobranching, primary root tips were grown to different lengths in air-gap (0 to 5 mm) and recovery (up to 2 mm in moist agar) conditions. (**J** and **K**) Emission ratio images (J) and box plots (K) of nlsABACUS2-400n reveal dynamic changes in endogenous ABA levels as root tips grow across air gap and after recovery. Color scale represents emission ratios. *$P \leq 0.05$; ***$P \leq 0.001$; ns, nonsignificant changes.

ABA regulates xerobranching by closing plasmodesmata

Genetic and biosensor-based studies revealed that ABA moves from its inner root (phloem) source to outer root tissues during a xerobranching response (Fig. 1, E to H and J; Fig. 2; and Fig. 3B). However, it remains unclear which root tissue(s) ABA targets to repress lateral root development during a xerobranching response. To determine this, we attempted to rescue the xerobranching defect of the ABA response mutant *snrk2.2/2.3* by expressing the WT *SnRK2.2* sequence under a series of root-tissue and/or zone-specific promoters (Fig. 3,

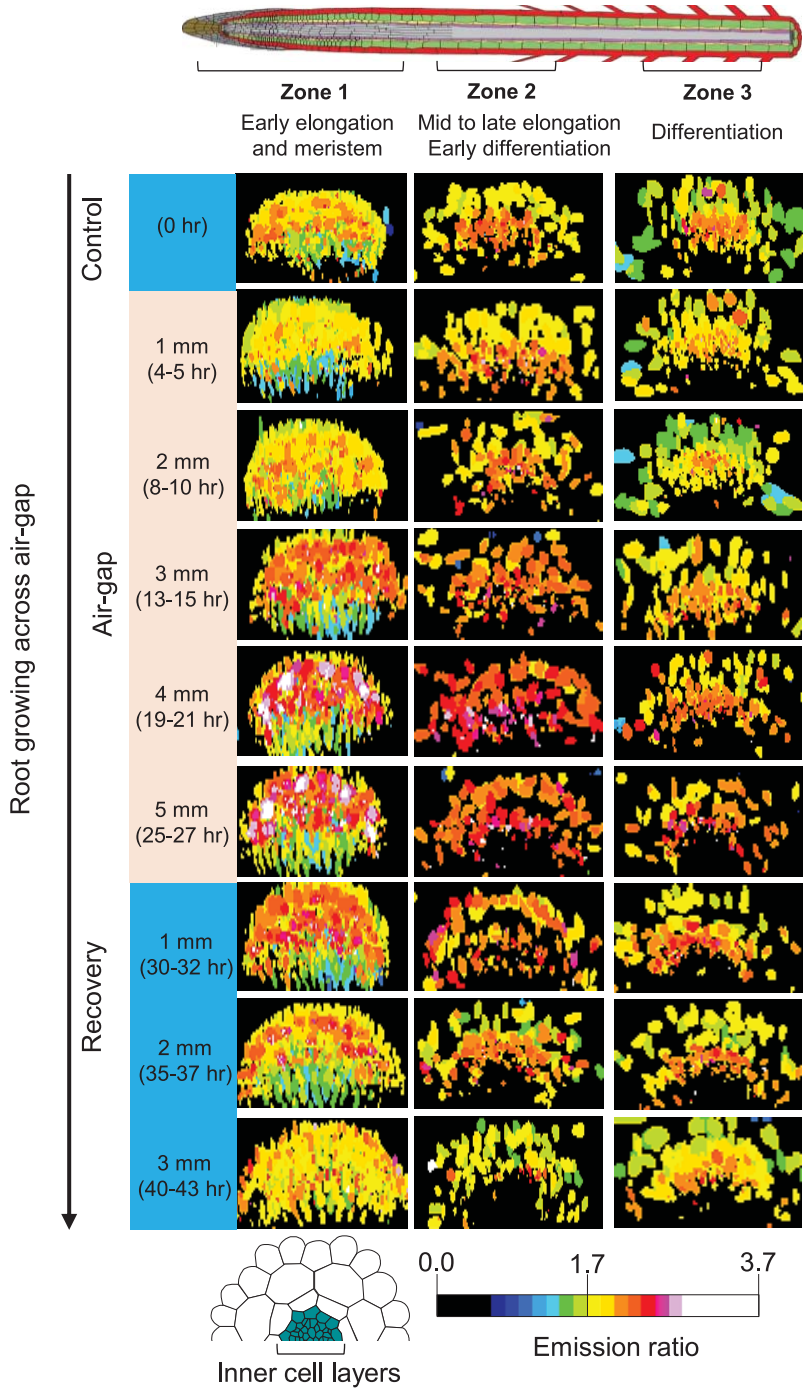

Fig. 2. ABA moves radially outward after a xerobranching stimulus. Ratio images of *Arabidopsis* roots expressing nlsABACUS2-400n reveal spatiotemporal distribution of ABA as the roots grow across an air gap. Each image is a representative maximum projection ratio map generated from a stack of several radial cross sections. Roots were imaged at different time points (indicated with hours) as they exit moist agar (control), grow in a 5-mm air gap, and reconnect with agar (recovery). Length (in millimeters) on the vertical axis indicates the length of root tips in air-gap and recovery conditions. For each time point, cross sections were generated from different zones of roots marked as zone 1 (early elongation and meristem), zone 2 (mid- to late elongation and early differentiation), and zone 3 (differentiation). Radial cross sections from zone 1 (compare cross sections from 1 to 5 mm) reveal an increase in ABA in outer (but not inner) tissues, which appears to originate from phloem unloading in zone 2 after a xerobranching stimulus. Color scale represents FRET emission ratios. Higher ratios correspond to higher ABA concentrations. Experiment was performed with at least four replicates per time point per zone (n = 4).

E to J). Expressing *SnRK2.2* in either root epidermal, cortical, endodermal, or basal meristem (but not lateral root cap) tissues rescued the *snrk2.2/2.3* xerobranching defect (Fig. 3, E to J). This result led us to ask, is there a common target important for xerobranching that the ABA signaling pathway regulates in each of these outer root tissues? ABA modulates hydraulic conductivity by inducing aquaporin expression to affect water movement out of the vasculature (*22*). To investigate possible roles of aquaporins in ABA-dependent repression of branching in air gaps, we analyzed a *pip* (plasma membrane intrinsic proteins) quadruple mutant in our xerobranching bioassay system. However, analysis of the *pip* mutant disrupting the most highly expressed *PIP* genes in roots did not show any significant difference compared with the WT control (fig. S14).

ABA has been reported to trigger reversible closure of intercellular pores, termed plasmodesmata (PD) (*23*). Does ABA regulate the xerobranching response by gating PD between root tissues? To address this, the symplastic fluorescent tracer carboxyfluorescein (CF) [derived from carboxyfluorescein diacetate (CFDA)] was used to monitor whether PD were open or shut in root tissues during a xerobranching response. Within plant cells, nonfluorescent CFDA is cleaved by cellular esterases to release membrane-impermeable fluorescent CF that travels exclusively through the PD. After CFDA application to cotyledons, we observed decreased protophloem unloading in *Arabidopsis* WT root tips that were exposed to a xerobranching stimulus (fig. S15). Delayed unloading was also observed in root tips of a *pSUC2:GFP* line that expresses free GFP in phloem companion cells (fig. S16). Collectively, both lines of evidence reveal that root tips experience decreased PD permeability after a xerobranching stimulus.

To assess the role of ABA in root PD gating during xerobranching, CFDA was locally applied to root tips. WT roots exhibited reduced intercellular fluxes of the tracer, which indicated closed PD after a xerobranching stimulus (Fig. 4, A and B). By contrast, CFDA treatment of root tips of the ABA response mutant *snrk2.2/2.3* revealed that PD remained open after a xerobranching stimulus (fig. S17). PD aperture is regulated by modifying the size of a callose ring encircling each end of the intercellular pore. The callose stain aniline blue revealed higher callose deposition in basal meristem cells of WT roots compared with *snrk2.2/2.3* after a xerobranching stimulus (fig. S18). Taken together, the evidence indicates that ABA regulates gating of PD in key root tissues during a xerobranching response.

To determine the function of PD gating during a xerobranching response, *Arabidopsis* mutants no longer able to gate their PD were characterized (figs. S19 and S20). PD aperture

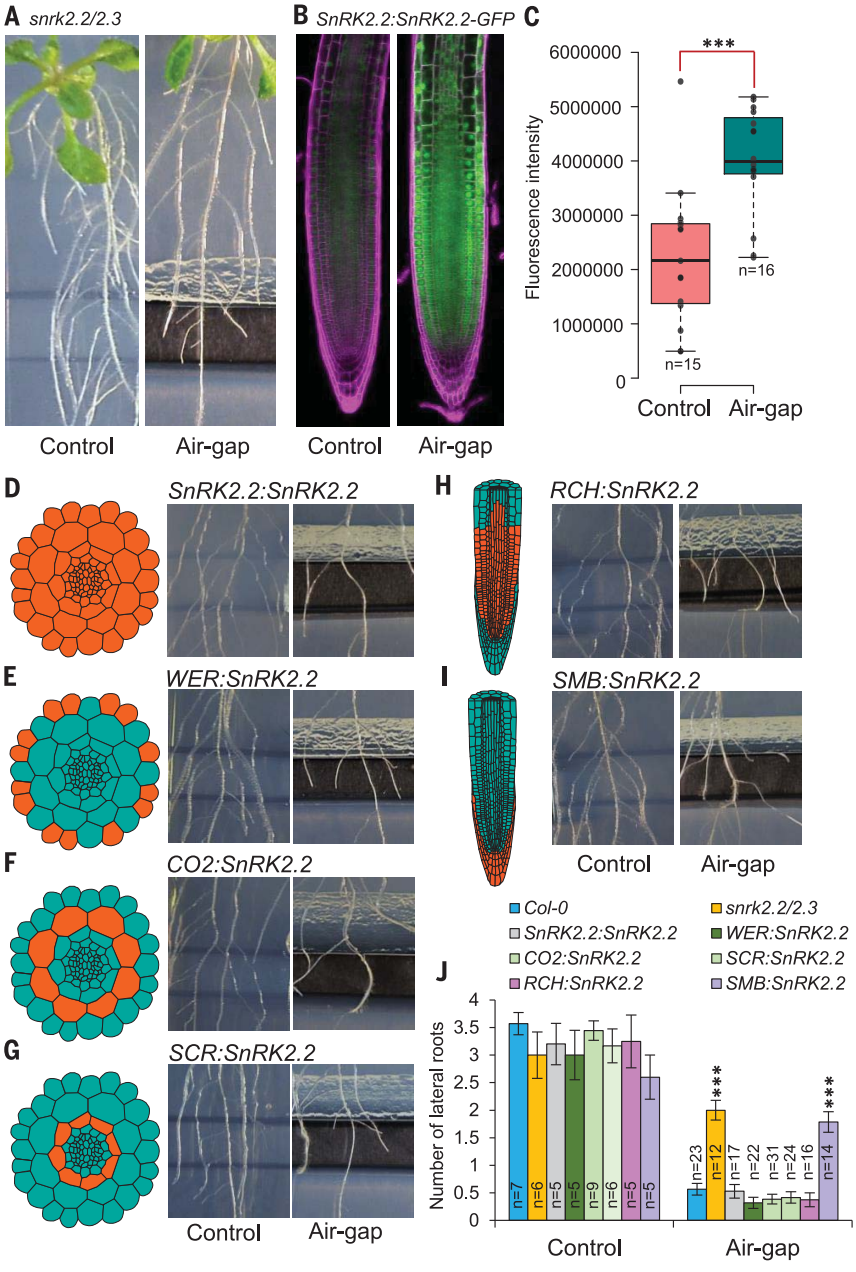

Fig. 3. Xerobranching is dependent on ABA perception in *Arabidopsis* primary root transition zone tissues. (**A**) ABA signaling mutant *snrk2.2/2.3* disrupts xerobranching in agar-based air-gap assay system. Air gap, ~5 mm. (**B** and **C**) Elevated response of *pSnRK2.2:SnRK2.2-GFP* in root tips subjected to air-gap versus control conditions. Scale bar, 100 μm. (**D**) Expression of *SnRK2.2* under its own promoter rescues the xerobranching defect of *snrk2.2/2.3*. (**E** to **G**) Functional complementation of *snrk2.2/2.3* by tissue-specific expression of *SnRK2.2* in epidermis, cortex, and endodermis using the *WER*, *CO2*, and *SCR* promoters, respectively. (**H**) Root zone–specific expression of *SnRK2.2* in root meristem and transition zone (using *RCH* promoter) rescues the xerobranching defect of *snrk2.2/2.3*. (**I**) Expression of *SnRK2.2* in columella and lateral root cap using SMB promoter in *snrk2.2/2.3* background. (**J**) Number of lateral roots produced by WT (Col-0), *snrk2.2/2.3*, and different tissue- and/or zone-specific rescue lines in the air-gap region versus the corresponding region of roots grown under control conditions. Orange color in root schematics defines the tissue and/or zone of expression of selected promoters used for complementation. Significant changes with respect to control (C) or WT (J) were calculated by Student's *t* test. ***$P \leq 0.001$.

is regulated through the action of enzymes, including a family of callose synthases and associated regulatory proteins such as PD-located proteins (PDLPs) (*24*). Mutating individual members of the *Arabidopsis* callose synthase gene family resulted in nine of these lines exhibiting a xerobranching defect, including *CALS7*, which is primarily associated with phloem sieve pores (fig. S19) (*25*), as did mutating both *PDLP2* and *PDLP3* genes (fig. S20). Hence, blocking the ability to close PD disrupts a root's ability to activate a xerobranching response.

How does ABA trigger PD closure after a xerobranching stimulus? Transgenic lines expressing GFP reporters that were fused to either PDLP2 or PDLP3 proteins under their native promoters were up-regulated in response to a xerobranching stimulus (Fig. 4, C and D, and figs. S21 to S23). In the case of PDLP3, its mRNA and *PDLP3:PDLP3-GFP* reporter were up-regulated in root tip and, specifically, basal meristem cells during a xerobranching response, exhibiting a punctate pattern in apical, basal, and side walls, consistent with its PD regulatory function (Fig. 4, C and D, and figs. S21 and S23). Treating roots of *PDLP3:PDLP3-GFP* with low levels of ABA (50 nM) phenocopied a xerobranching stimulus (fig. S24), in agreement with the presence of several ABA-responsive elements (ABREs) in its promoter sequence (table S1). We also noted that many other *PDLP* and *callose synthase* genes contained ABREs in their promoter sequences (tables S1 and S2). Comparing spatiotemporal response curves of nlsABACUS2 and PDLP3-GFP (during xerobranching and subsequent recovery) reveals that ABA accumulation precedes PDLP3 induction (Fig. 1K and fig. S23). To test the functional importance of ABA-regulated PDLP up-regulation during xerobranching, we characterized the ABA-insensitive mutant *abi1-1*. The dominant negative *abi1-1* allele disrupts ABA-dependent PD closure and maintains high frequencies of open PD (*26*). Unlike WT, *abi1-1* roots exhibit branching in air gaps (fig. S25). However, ectopic expression of *PDLP1* (using *35S* rather than its native promoter) rescued the xerobranching defect of *abi1-1* (fig. S25). Hence, ABA triggers PD closure after a xerobranching stimulus by up-regulating expression of *PDLP*s. Additionally, GAL4-mediated transactivation of *abi1-1* in root ground tissues (cortex and endodermis) led to maximal disruption of xerobranching response as compared with induction of *abi1-1* in single root cell layers (fig. S26). Hence, ABA-mediated PD closure in root ground tissues is essential for a xerobranching response.

PD closure blocks inward auxin movement

How does ABA-mediated PD gating disrupt lateral root branching? Our reporter studies reveal that closing PD during a xerobranching response blocks the inward (symplastic) movement of another plant hormone signal, auxin, which is required to initiate lateral root branching. Exposing roots of the *DR5:VENUS* auxin reporter line to a xerobranching stimulus results in an elevated auxin response in epidermal cells within the root basal meristem zone (Fig. 4, E and F). The altered *DR5:VENUS* reporter pattern is consistent with xerobranching-induced PD closure in basal meristem epidermal cells transiently blocking the radially inward symplastic movement of auxin (Fig. 4, E and F, and fig. S27).

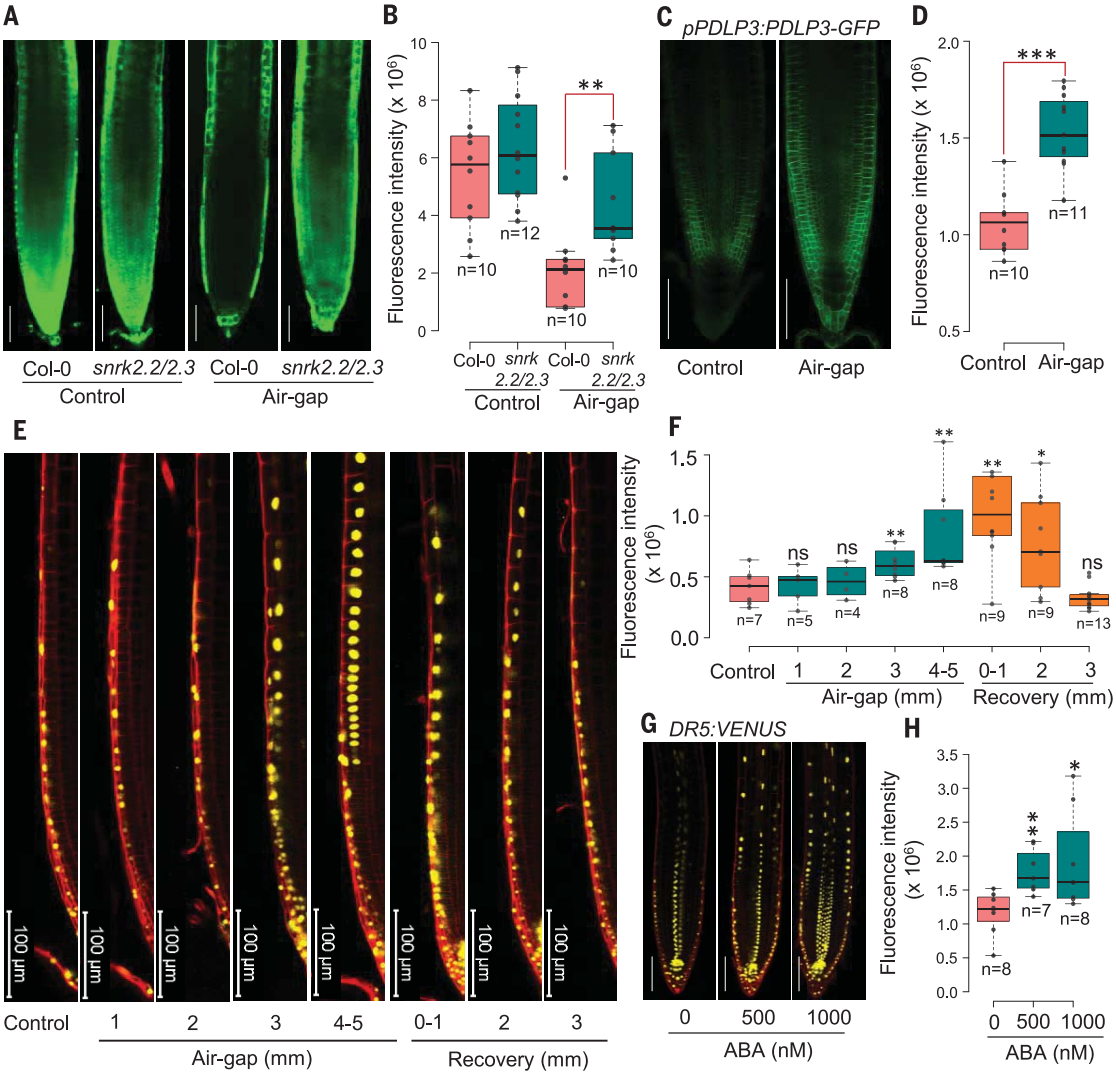

Fig. 4. ABA blocks radial auxin flow by reducing PD permeability causing xerobranching. (**A**) Slower migration of symplastic tracer CF in WT *Arabidopsis* (Col-0) primary root tips subjected to xerobranching stimulus versus control conditions. CF migration was indistinguishable in ABA signaling mutant *snrk2.2/2.3* with or without the xerobranching stimulus. Root tips were treated with CFDA before imaging. (**B**) CF fluorescence intensity in WT and *snrk2.2/2.3* root tips exposed to air-gap versus control conditions. (**C**) Xerobranching stimulus induces expression of *pPDLP3:PDLP3-GFP*. (**D**) Box plots showing significantly enhanced response of *pPDLP3:PDLP3-GFP* in air-gap versus control conditions. (**E** and **F**) Auxin response reporter *DR5:VENUS* shows higher fluorescence signal in epidermis of root tips exposed to air-gap versus control and recovery conditions. (**G** and **H**) ABA treatments phenocopy *DR5:VENUS* response during xerobranching. Scale bar, 100 µm. *$P \leq 0.05$; **$P \leq 0.01$; ***$P \leq 0.001$; ns, nonsignificant (Student's *t* test).

The auxin reporter DII-VENUS also revealed higher auxin abundance in root tips during exposure to a xerobranching stimulus (figs. S27 and S28). The effect of a xerobranching stimulus on *DR5:VENUS* and DII-VENUS can be mimicked by exogenous application of ABA to roots (Fig. 4, G and H, and fig. S29). ABA-mediated PD gating during a xerobranching response blocks radial inward auxin movement and lateral root induction. Consistent with this model, switching off ABA signaling in the *abi1-1* mutant (which ensured that PD remained constitutively open) blocked any change in DII-VENUS auxin response after a xerobranching stimulus (fig. S30). Suppression of lateral root initiation in roots exposed to a xerobranching stimulus was visualized by using the *DR5:LUC* reporter, which normally demarks groups of lateral root stem cells in the basal meristem (or oscillation zone) that go on to form new branches in control roots, but these *DR5:LUC* oscillations were blocked in roots exposed to a xerobranching stimulus (fig. S31). Hence, the xerobranching response blocks radially inward symplastic auxin movement that is required for lateral root induction.

Root auxin distribution was originally thought to be exclusively determined by the combined activities of AUX1/LAX, ABCB, and PIN auxin influx and efflux carriers (*27*). To determine the impact of xerobranching on carrier-mediated auxin transport, reporter lines for key auxin influx (*pAUX1:AUX1-YFP*) or efflux (*pPIN2:PIN2-GFP*) carriers expressed in the root elongation zone were analyzed (fig. S32). No spatial changes were detected in AUX1-YFP or PIN2-GFP expression in the outermost root tissues after a xerobranching stimulus, consistent with the observed elevated auxin response (Fig. 4, E and F, and fig. S27) being the result of gating of hormone movement through PD rather than through modulation of apoplastic auxin transport (fig. S32). Ectopic expression of either *AUX1* or *PIN2* in every elongation zone tissue, to create a synthetic radial apoplastic auxin pathway, successfully bypassed the PD-mediated restriction of symplastic auxin flow and led to lateral root branching in air gaps (fig. S33).

Collectively, multiple lines of evidence establish a role for ABA-mediated PD gating of radial symplastic auxin flow to regulate xerobranching. Roots appear to sense water availability by comobilizing water and hormones through PD. If water, ABA, and auxin moved through substrate-specific carriers (aquaporins, ABCG, and PINs), their comobilization would be broken. Instead, because PD are large intercellular pores that are nonselective, radial hydraulic fluxes comobilize hormones either inward (such as auxin) or outward (such as ABA) when water is available or not, respectively. Thus, auxin and ABA can be considered as hydrosignals when comobilized through PD with water.

Our study has revealed that xerobranching is a widely conserved, ABA-dependent root adaptive response to localized loss of contact with soil water in eudicot and monocot species. We also report the molecular and cellular mechanisms that enable plant roots to block lateral root formation after experiencing a xerobranching stimulus (see schematic in Fig. 5). Under optimal moisture conditions,

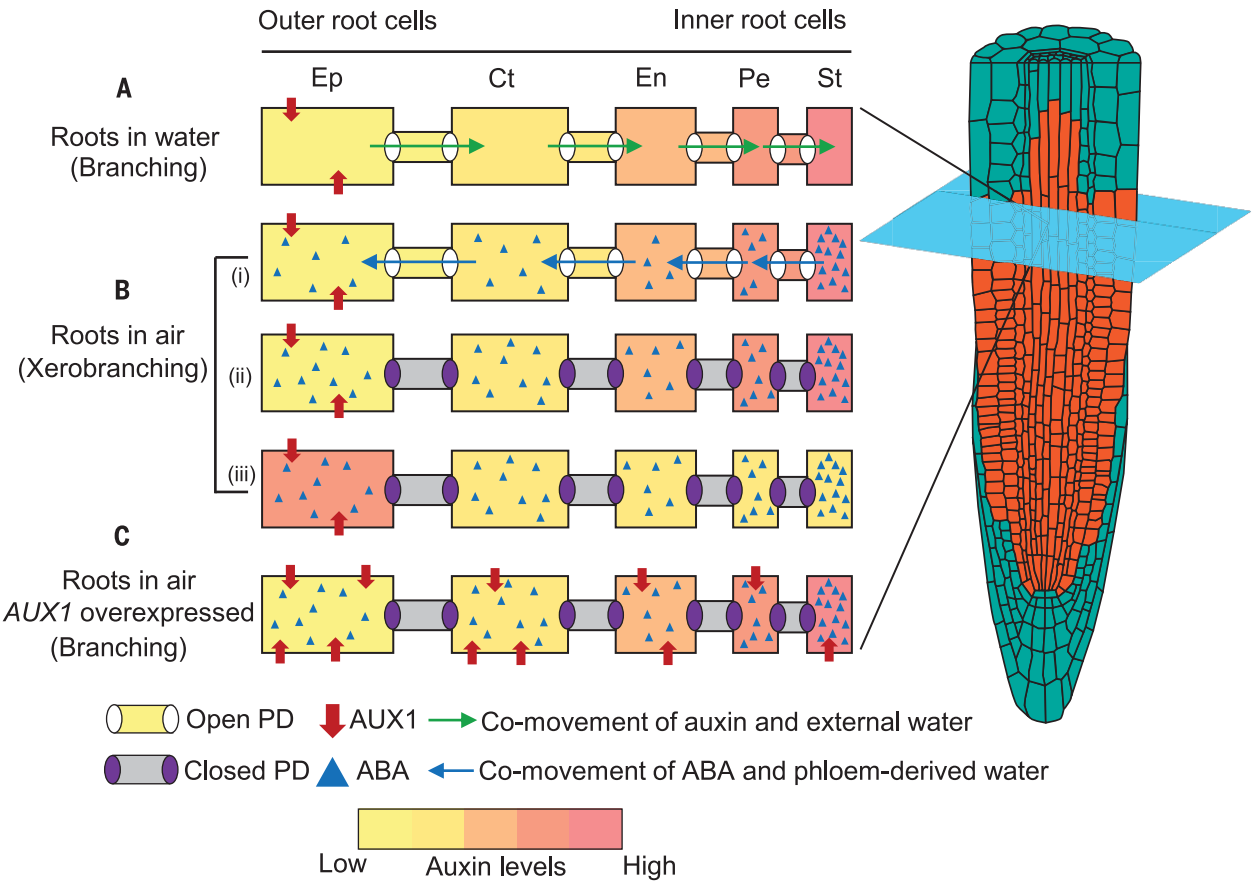

Fig. 5. Dynamic hormone redistribution determines root branching or xerobranching response to external water availability. Schematics illustrate cellular auxin, ABA, and water fluxes in root basal meristem (highlighted cell files in transverse root section) exposed to water or air. (**A**) Under normal moisture conditions, roots cotransport water and auxin radially inward through PD, which delivers the key hormone signal (auxin) to pericycle cells, where lateral root initiation is triggered. (**B**) Xerobranching stimulus triggers rise in ABA levels in inner root tissues (stele), which suppresses root branching. In the transient absence of external water, phloem-derived water comobilizes ABA from inner (stele) to outer root cells (epidermis) through PD (i). ABA induces closure of PD through *PDLP*s and *CALs* (ii) disrupting symplastic radial movement of auxin to pericycle (iii). (**C**) Ectopic expression of auxin carriers such as AUX1 in all elongation zone tissue creates a synthetic radial apoplastic auxin pathway, which bypasses the disrupted symplastic auxin flow and thus causes root branching in air gap. Ct, cortex; En, endodermis; Ep, epidermis; Pe, pericycle; St, stele.

roots cotransport auxin and water inward between root basal meristem tissues through PD and thus provide a symplastic pathway to radially mobilize this key hormone signal with hydraulic fluxes from epidermal to pericycle cells, where auxin triggers lateral root initiation. However, when the external source of water is transiently unavailable, root tips rely on an internal (phloem) source of water to continue growing (*15*) and couple its outward radial flow with movement of the hormone ABA. This key water stress signal reduces PD aperture, disrupting radial movement of the branching signal auxin to lateral root "stem cells" in the pericycle. Restoring an external water source (during the recovery phase) rapidly reduces ABA levels in the outermost root tissues (>3 hours) and thus restores open PD and symplastic auxin transport. Once reconnected with an external water source, the abundance and distribution of these signals reset in root-tip tissues to pre–xerobranching-stimulus levels. These dynamic regulatory events—coupling changes in hydraulic fluxes with hormone redistribution, which we term hydrosignaling—enable plant roots to calibrate spatial root branching responses in heterogeneous soil environments, which are the norm rather than the exception. Climate change is likely to exacerbate water scarcity (*9*, *10*); thus, that water in soils will be even more heterogeneously distributed in the future than at present is highly likely. Insight into the molecular and cellular mechanisms through which roots acclimate under these conditions may improve the climate resilience of future crops.

REFERENCES AND NOTES

1. B. Muller *et al.*, *Trends Plant Sci.* **24**, 810–825 (2019).
2. J. P. Lynch, *Plant Physiol.* **156**, 1041–1049 (2011).
3. H. Motte, T. Beeckman, *J. Exp. Bot.* **70**, 785–793 (2019).
4. E. C. Morris *et al.*, *Curr. Biol.* **27**, R919–R930 (2017).
5. A. Zhan, H. Schneider, J. P. Lynch, *Plant Physiol.* **168**, 1603–1615 (2015).
6. R. Karlova, D. Boer, S. Hayes, C. Testerink, *Plant Physiol.* **187**, 1057–1070 (2021).
7. B. Orman-Ligeza *et al.*, *Curr. Biol.* **28**, 3165–3173.e5 (2018).
8. Y. Bao *et al.*, *Proc. Natl. Acad. Sci. U.S.A.* **111**, 9319–9324 (2014).
9. D. B. Lobell, S. M. Gourdji, *Plant Physiol.* **160**, 1686–1697 (2012).
10. Y. Grusson, I. Wesström, E. Svedberg, A. Joel, *Agric. Water Manage.* **249**, 106766 (2021).
11. A. J. Thompson *et al.*, *Plant Cell Environ.* **27**, 459–471 (2004).
12. I. B. Taylor, R. S. T. Linforth, R. J. Al-Naieb, W. R. Bowman, B. A. Marples, *Plant Cell Environ.* **11**, 739–745 (1988).
13. B. C. Tan, S. H. Schwartz, J. A. D. Zeevaart, D. R. McCarty, *Proc. Natl. Acad. Sci. U.S.A.* **94**, 12235–12240 (1997).
14. T. Kuromori, E. Sugimoto, K. Shinozaki, *Plant Physiol.* **164**, 1587–1592 (2014).
15. B. S. Wiegers, A. Y. Cheer, W. K. Silk, *Plant Physiol.* **150**, 2092–2103 (2009).
16. V. Couvreur *et al.*, *Plant Physiol.* **178**, 1689–1703 (2018).
17. F. C. Pascut *et al.*, *Nat. Commun.* **12**, 4682 (2021).
18. J. Rowe *et al.*, bioRxiv 2022.10.19.512731 [Preprint] (2022).
19. T. J. Ross-Elliott *et al.*, *elife* **6**, e24125 (2017).
20. I. De Smet *et al.*, *Development* **134**, 681–690 (2007).
21. M. A. Moreno-Risueno *et al.*, *Science* **329**, 1306–1311 (2010).
22. K. Prado *et al.*, *Plant Cell* **25**, 1029–1039 (2013).
23. Y. Benitez-Alfonso, *Plant Cell Physiol.* **60**, 713–714 (2019).
24. C. L. Thomas, E. M. Bayer, C. Ritzenthaler, L. Fernandez-Calvino, A. J. Maule, *PLOS Biol.* **6**, e7 (2008).
25. B. Xie, X. Wang, M. Zhu, Z. Zhang, Z. Hong, *Plant J.* **65**, 1–14 (2011).

26. S. Tylewicz *et al*., *Science* **360**, 212–215 (2018).
27. J. Petrášek, J. Friml, *Development* **136**, 2675–2688 (2009).

ACKNOWLEDGMENTS

We thank P. L. Rodriguez (CSIC-UPV, Spain) for sharing *pyr/pyl1124589*, *pyr/pyl1124578*, and *pyr/pyl112458* mutants; H. Fujii (University of Turku, Finland) for sharing *snrk2.2/3/6*, *snrk2.1/4/5/7/8/9/10*, and *snrk2.1/3/4/5/6/7/8/9/10* mutants; and R. Miao (Fujian Agriculture and Forest University, China) for sharing *hab1-1abi1-2pp2ca*, *hab1-1abi1-2abi2-2*, and *Qabi2-2* mutants. We thank L. Kalmbach, Y. Helariutta (SLCU, UK), and N. Geldner (University of Lausanne, Switzerland) for sharing *pSUC2:GFP* seeds. We also thank Z. Gong and Y. Wang (China Agricultural University) for kindly sharing *abi1-1* (Col-0) seeds. We acknowledge C. Luschnig (University of Natural Resources and Life Sciences – BOKU, Vienna) and J. Friml (IST, Austria) for sharing *eir1-4/PIN2:PIN2-GFP* and *eir1-4/35S:PIN2-GFP* lines. We thank F. Augstein and A. Carlsbecker (Uppsala University, Sweden) for providing *UAS:abi1-1* and driver lines. We thank F. Chaumont (Louvain-la-Neuve, Belgium) and A. Schäffner (Helmholtz Zentrum München, Germany) for sharing the aquaporin mutant. **Funding:** This study was supported by a European Molecular Biology Organization Long-Term Fellowship (ALTF 1140-2019 to P.M.); European Union's Horizon 2020 research and innovation program, Marie Skłodowska-Curie, XEROBRANCHING (891262 to P.M.); Biotechnology and Biological Sciences Research Council Discovery Fellowship (BB/V00557X/1 to B.K.P.); the Biotechnology and Biological Sciences Research Council (BB/T001437/1 to M.J.B. and A.S.; BB/V003534/1 to M.J.B., A.S., and J.B.; BB/W008874/1 to M.J.B. and C.J.S.; BB/W015080/1 to M.J.B.; and BB/P018572/1 to A.M.J.); European Research Council grant FUTUREROOTS (294729 to M.J.B.); European Research Council, SUMOrice (grant no. 310235 to A.S.); Fonds de la Recherche Scientifique – FNRS (to V.C.); the Swedish Research Council (no. 2020-03522 to R.P.B.); European Research Council, RobustHormoneTrans (757683 to E.S.); the NSF Plant Genome Research Program (IOS-1444448 to R.E.S.); the Gatsby Charitable Foundation (to A.M.J. and J.R.); European Research Council grant INTERCELLAR (725459 to C.F.); and the Biotechnology and Biological Research Council Institute Strategic Programme, Plant Health (BBS/E/J/000PR9796 to C.F.).

Author contributions: Conceptualization: P.M. and M.J.B. Methodology: P.M., B.K.P., V.C., J.R., and H.D.G. Investigation: P.M., B.K.P., D.M., J.B., N.L., V.C., J.R., M.A., H.D.G., E.M., C.J.S., and R.S. Funding acquisition: P.M. and M.J.B. Supervision: M.J.B. Writing – original draft: M.J.B. and P.M. Writing – review & editing: P.M., B.K.P., D.M., J.B., N.L., V.C., J.R., M.A., H.D.G., E.M., C.J.S., R.S., S.J.M., C.F., T.B., R.P.B., E.S., A.M.J., I.C.D., R.E.S., A.S., X.D., and M.J.B. **Competing interests:** The authors declare no competing interests. **Data and materials availability:** No restrictions are placed on materials, such as materials transfer agreements. All data are available in the main text or the supplementary materials.

SUPPLEMENTARY MATERIALS

science.org/doi/10.1126/science.add3771
Materials and Methods
Figs. S1 to S33
Tables S1 and S2
References (*28*–*59*)
MDAR Reproducibility Checklist

View/request a protocol for this paper from *Bio-protocol*.

Submitted 8 June 2022; accepted 24 October 2022
10.1126/science.add3771

Science

Hydraulic flux–responsive hormone redistribution determines root branching

Poonam MehraBipin K. PandeyDalia MelebariJason BandaNicola LeftleyValentin CouvreurJames RoweMoran AnfangHugues De GernierEmily MorrisCraig J. SturrockSacha J. MooneyRanjan SwarupChristine FaulknerTom BeeckmanRishikesh P. BhaleraoEilon ShaniAlexander M. JonesIan C. DoddRobert E. SharpAri SadanandomXavier DrayeMalcolm J. Bennett

Science, 378 (6621), • DOI: 10.1126/science.add3771

Lateral root development

Plant roots are most effective in pockets of soil containing the water that the plant needs. Water is not uniformly distributed throughout the soil, and the xerobranching response, in which lateral root formation is suppressed, ensures that roots are not uniformly distributed either. Mehra *et al*. show what happens as plant roots grow into and through dry pockets in soil. In moist conditions, water flows from the root surface into the phloem, but in a dry spot, water flows instead from the phloem out into the root tissues. This reverse flow carries along the phloem-derived hormone abscisic acid, which closes off intercellular pores, blocking the ability of the hormone auxin to initiate lateral root development. —PJH

Science (ISSN) is published by the American Association for the Advancement of Science. 1200 New York Avenue NW, Washington, DC 20005. The title *Science* is a registered trademark of AAAS.